

Quantum ferroelectric instabilities in superconducting SrTiO₃

J. R. Arce-Gamboa¹, G. G. Guzmán-Verri^{1,2}

¹*Materials Research Science and Engineering Center,
University of Costa Rica, San José, Costa Rica 11501, and*

²*Materials Science Division, Argonne National Laboratory, Argonne, Illinois, USA 60439,*

(Dated: January 30, 2018)

Recent experiments on doped SrTiO₃ have shown that superconductivity is favored by its proximity to a quantum ferroelectric instability,^{1,2} suggesting that pairing between its charge carriers could be promoted by quantum criticality.³ Here, we consider a model that combines a strong coupling theory of superconductors with a standard framework for the soft polar modes in SrTiO₃ including their coupling to strain degrees of freedom, lattice dimensionality, displacive nature, and the long-ranged and anisotropic dipolar interactions, which are usually neglected. Our calculations of the superconducting temperature T_c for several applied stresses and cation substitutions reveal that while quantum criticality favors superconductivity, optimal doping is not necessarily pinned to the quantum critical point. We qualitatively reproduce the observed reduction of T_c with hydrostatic pressure^{4,5} and use our model to gain insight into the aforementioned experiments.

I. INTRODUCTION

Strontium titanate (STO) is the first superconducting oxide to be discovered more than half-a-century ago.⁶ Upon doping, it exhibits dome-shaped superconductivity⁷⁻¹⁰ similar to the well-known cuprates at unusually low charge carrier concentrations (10^{15} cm^{-3}),¹¹⁻¹⁴ dubbing STO as the most dilute superconductor.¹⁵ Since its observation, the origin of the pairing mechanism between its charge carriers has posed a long-standing problem in condensed matter physics, as the conventional Bardeen-Cooper-Schrieffer theory of superconductors requires the so called adiabatic limit of electron-phonon coupling in which the characteristic energy scale of the charge carriers (the Fermi temperature T_F) is much larger than that of the phonons (the Debye temperature T_D).¹⁶ STO is unusual in that it is outside this limit as $T_F \simeq 13 \text{ K}$ ¹⁵ and $T_D \simeq 400 \text{ K}$.¹⁷ Though several models have been put forward,¹⁸⁻²⁰ there is still no consensus on the pairing mechanism between its charge carriers.

Recently, Edge et al.³ have proposed a quantum critical origin for superconductivity in STO. Within this framework, a superconducting dome arises in STO because a quantum critical point (QCP) that separates competing ferroelectric (FE) and paraelectric (PE) ground states generates soft transverse optic (TO) phonons which favor the formation of Cooper pairs between charge carriers by increasing the superconducting coupling constant λ between them at low densities. With increasing doping, the frequency of the phonons hardens, which decreases λ and therefore T_c as well, despite more carriers are available to superconduct. The proposal is inspired from extensive work on strongly correlated electron systems^{21,22} such as heavy fermion materials and the cuprates where it has been proposed that competing phases close to a quantum critical point lead to highly collective low energy excitations, such that any residual interactions drive the system to a new phase such as superconductivity.

Though STO is not within the adiabatic limit,²³ the model provides a good description of its superconducting dome and it has received recent experimental support.^{1,2}

In conventional FEs, the relevant low energy lattice excitations are zone-center TO phonons which break spatial inversion symmetry and trigger a phase with a spontaneous, reversible polarization upon condensation. In pure STO, such transition is aborted by quantum fluctuations of the polarization order parameter²⁴ and, instead, incipient FE behavior is observed in which the dielectric constant grows enormously ($\simeq 10^4$) and the phonon frequencies soften down to lowest observed temperatures without condensing.²⁵ Long-range FE order can be induced by tensile stress,²⁶ oxygen isotope exchange,²⁷ or cation substitution.²⁸ At the QCP, the phonon excitations become gapless and at finite temperatures above it but well below T_D ,²⁹ quantum criticality sets in generating unusual behavior, such as a T^{-2} dependence in the dielectric susceptibility distinct from that of the neighboring PE and FE phases.³⁰

To model the phonon excitations that mediate the pairing between carriers, one-dimensional transverse Ising models with short-range interactions are invoked and solved within a mean field approximation.^{3,31,32} Such models describe order-disorder FEs, but do not apply to STO, which exhibits typical displacive behavior, a low-temperature pseudocubic phase, and a transition driven by long-range anisotropic dipolar interactions.³³ The aim of this paper is to address the roles of all of these on the superconducting phase of doped STO by combining a standard model for displacive FEs which includes coupling between the polar and long-wavelength strain generating acoustic modes.

We make use of a self-consistent phonon approximation (SCPA) to study the quantum statistical mechanics of our model Hamiltonian which includes local thermal and quantum fluctuations of the order parameter.³⁴ This allows us to calculate the doping and stress dependence of the superconducting and ferroelectric transition temperatures (T_{fe}) self-consistently as well as the doping,

stress and temperature dependence of the phonon frequencies and the order parameter. Crucially, we make no a-priori assumption about quantum criticality. We find that proximity to quantum criticality favors superconductivity, but, unlike one-dimensional models, the optimal T_c is not pinned to the QCP unless very large tensile stresses are applied or large concentrations of Sr are substituted by cations that favor long-range FE order such as Ca, which can be experimentally tested. Our model qualitatively accounts for the recent observation of coexistent FE-like and superconducting instabilities in n-doped Ca-substituted SrTiO₃ (Sr_{1-x}Ca_xTiO₃, STO:Ca-x).²

II. MODEL

Following Ref. [3], our starting point is the McMillian formula³⁵ for the superconducting coupling constant,

$$\lambda(T, \sigma) = \int_0^\infty \alpha_{e-ph}^2(\omega) D(\omega) \frac{d\omega}{\omega},$$

where $\alpha_{e-ph}(\omega)$ is the electron-phonon coupling that depends on the frequency ω of the phonon excitation. $D(\omega)$ is the phonon density of states. For the soft modes, $D(\omega) = \sum_{\mathbf{q}, \mu} \delta(\omega - \Omega_{\mathbf{q}\mu})$, where $\Omega_{\mathbf{q}\mu}$ are the soft phonons. Assuming α is independent of ω , we obtain,

$$\lambda(T, \sigma) = \alpha_{e-ph}^2 \sum_{\mathbf{q}, \mu} \frac{1}{\Omega_{\mathbf{q}\mu}}. \quad (1)$$

where the sum over \mathbf{q} runs over the entire Brillouin zone and the sum over $\mu = 1, 2, 3$ is over the optic phonon modes.

T_c is calculated from the strong-coupling theory,³

$$1 = \frac{\lambda(T_c, \sigma)}{2\pi^2} \int_{-\epsilon_F}^0 d\epsilon N(\epsilon) \frac{\tanh(\beta_c \epsilon/2)}{\epsilon}, \quad (2)$$

where $N(\epsilon) \simeq \sqrt{\epsilon + \epsilon_F}$ is the electron density of states near the Fermi level ϵ_F , and $\beta_c = (k_B T_c)^{-1}$.

We now need a model for the phonon excitations. We consider a standard model Hamiltonian for displacive FEs with normal mode coordinates that describe local displacements $\mathbf{Q}_i = (Q_{ix}, Q_{iy}, Q_{iz})$ in the unit cell i that are associated with the soft TO mode, the condensation of which is driven by the dipolar force and leads to the FE transition.³³ We also consider elastic strains η_α as a secondary order parameter coupled to the primary order parameter \mathbf{Q}_i . We write the components of the strain tensor in the usual Voigt notation: $\eta_\alpha \equiv \epsilon_{\alpha\alpha} = \partial u_\alpha / \partial x_\alpha$ ($\alpha = 1, 2, 3$), $\eta_4 = 2\epsilon_{yz} = 2(\partial u_y / \partial z + \partial u_z / \partial y)$, $\eta_5 = 2\epsilon_{xz} = 2(\partial u_x / \partial z + \partial u_z / \partial x)$, and $\eta_6 = 2\epsilon_{xy} = 2(\partial u_x / \partial y + \partial u_y / \partial x)$.

The Hamiltonian is as follows,³⁴

$$H = H_Q + H_\eta + H_{Q\eta}, \quad (3)$$

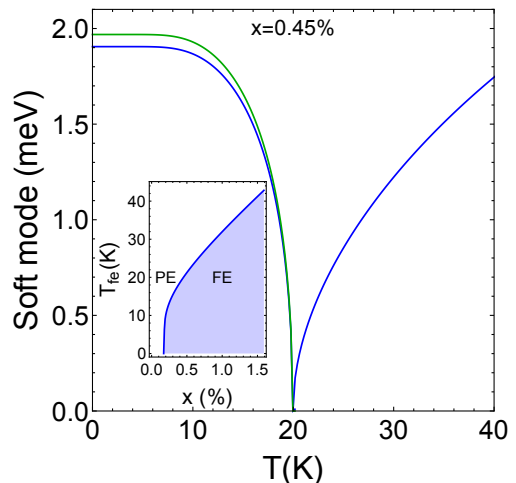


FIG. 1. Calculated TO soft mode frequencies for STO:Ca-0.45% showing the expected split of the high-temperature TO doublet into two modes at the FE transition $T_{fe} \simeq 20$ K (blue and green lines). Inset: Calculated phase diagram for STO:Ca-x.

where,

$$H_Q = \frac{1}{2} \sum_i |\Pi_i|^2 + \frac{\kappa}{2} \sum_i |\mathbf{Q}_i|^2 + \frac{\alpha}{4} \sum_i |\mathbf{Q}_i|^4 + \frac{\gamma}{2} \sum_{i, \nu \neq \nu'} Q_{i\nu}^2 Q_{i\nu'}^2 - \frac{1}{2} \sum_{ij\nu\nu'} v_{ij}^{\nu\nu'} Q_{i\nu} Q_{j\nu'}, \quad (4a)$$

$$H_\eta = \frac{1}{2} \sum_{i, \alpha \beta=1}^6 C_{\alpha\beta} \eta_{\alpha i} \eta_{\beta i} - \sigma \sum_{i, \alpha=1}^3 \eta_{\alpha i}, \quad (4b)$$

TABLE I. Model parameters for doped STO:Ca-x.

ω_0^2	15.5	meV
α	7.9	meV \AA^{-4}
γ	13.8	meV \AA^{-4}
$B^2 a^2$	2100	meV ²
C^2	2.9	meV ²
b_1	5.0	meV
b_2	3.4×10^{-16}	
g	30.7	
Qa	π	
α_{e-ph}	1.5	meV ^{1/4} $\text{\AA}^{3/2}$
e_a	4.2	meV ²
e_t	0.1	meV ²
C_a	7.2×10^4	meV
C_t	4.6×10^4	meV

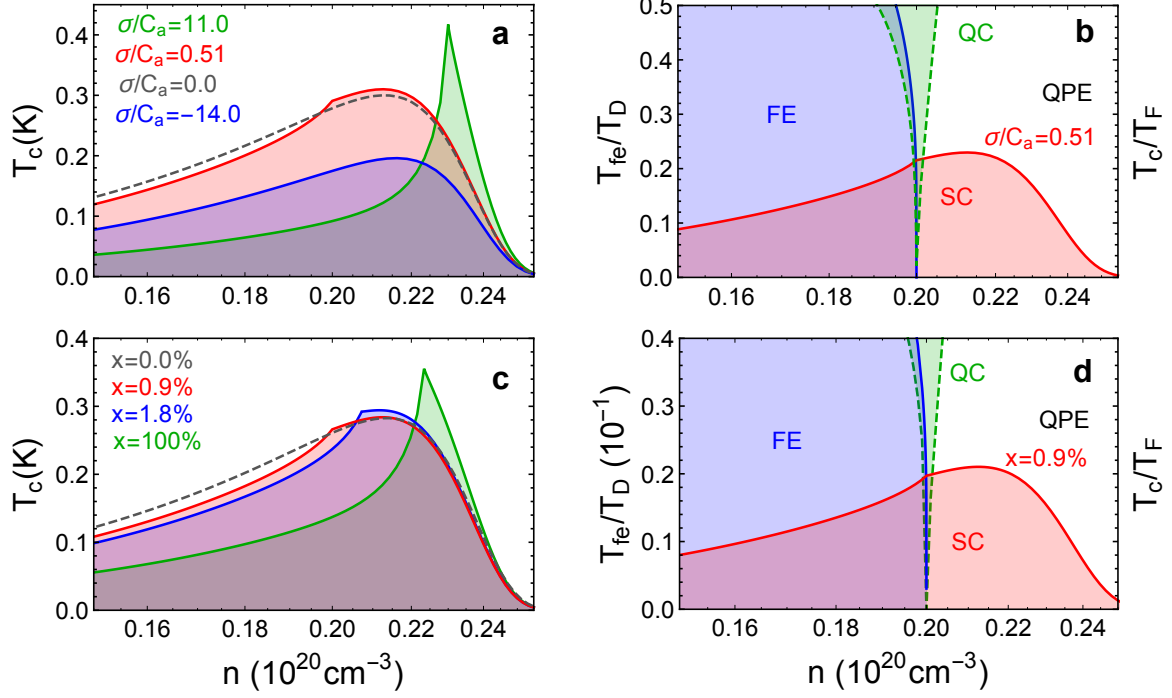


FIG. 2. (a) Calculated T_c for n-doped STO for several uniform stresses. The dome kink and peak for moderate (red) and strong (green) tensile stresses are due to the QCP located at the same charge carrier densities. (b) Calculated phase diagram for STO at $\sigma/C_a = 6.0$. (c) Calculated T_c for STO:Ca- x . (d) Phase diagram for $x = 0.9\%$. Green area corresponds to the QC region given by $\Omega < T \ll T_D$.

$$\begin{aligned}
H_{Q\eta} = & -e_a \sum_i (\eta_{1i} + \eta_{2i} + \eta_{3i}) |\mathbf{Q}_i|^2 \\
& - e_t \sum_i [\eta_{1i} (2Q_{ix}^2 - Q_{iy}^2 - Q_{iz}^2) \\
& \quad + \eta_{2i} (2Q_{iy}^2 - Q_{ix}^2 - Q_{iz}^2) \\
& \quad \quad + \eta_{3i} (2Q_{iz}^2 - Q_{ix}^2 - Q_{iy}^2)] \\
& - e_r \sum_i (Q_{ix}Q_{iy}\eta_{6i} + Q_{ix}Q_{iz}\eta_{5i} + Q_{iy}Q_{iz}\eta_{4i}),
\end{aligned} \quad (4c)$$

Here, $\mathbf{\Pi}_i$ is the conjugate momentum of \mathbf{Q}_i ; and $v_{ij}^{\nu\nu'}$ ($\nu, \nu' = x, y, z$) is the dipolar interaction tensor with Fourier transform $v_{\mathbf{q}}^{\nu\nu'} = [\frac{1}{3}C^2 - B^2|\mathbf{q}|^2] \delta_{\nu\nu'} - C^2 \frac{q_\nu q_{\nu'}}{|\mathbf{q}|^2}$, where $|\mathbf{q}| = \sqrt{q_x^2 + q_y^2 + q_z^2}$ is the magnitude of the wavevector \mathbf{q} ; and B and C are constants that depend on the lattice structure.³⁶ κ is the lattice stiffness; α and γ are coefficients of the isotropic and anisotropic cubic anharmonicities, respectively. e_a, e_t , and e_r are coupling constants between the polar and strain degrees of freedom; $C_{\alpha\beta}$ and σ are elastic constants and a uniform applied stress in units of energy, respectively (the usual elastic constants and homogeneous stresses are given by $C_{\alpha\beta}a^{-3}$ and σa^{-3} where a is the lattice constant).

We now study the quantum statistical mechanics of the Hamiltonian (3) within SCPA. We consider the PE and FE phases separately.

A. Paraelectric phase

In the PE phase the soft modes are a doubly degenerate transverse optic (TO) mode $\Omega_{\mathbf{q}}^{\perp}$, and a singlet longitudinal optic (LO) mode $\Omega_{\mathbf{q}}^{\parallel}$.³⁷ According to Eq. (1), we therefore have,

$$\lambda(T_c, \sigma) = \alpha_{e-ph}^2 \sum_{\mathbf{q}} \left(\frac{2}{\Omega_{\mathbf{q}}^{\perp}} + \frac{1}{\Omega_{\mathbf{q}}^{\parallel}} \right), \quad (5)$$

where,

$$(\Omega_{\mathbf{q}}^{\parallel})^2 = (\Omega_{\mathbf{q}}^{\perp})^2 + C^2, \quad (6a)$$

$$(\Omega_{\mathbf{q}}^{\perp})^2 = (\Omega_0^{\perp})^2 + B^2 |\mathbf{q}|^2. \quad (6b)$$

Ω_0^{\perp} is the TO mode at the zone-center and, within SCPA, it is given as follows,³⁴

$$(\Omega_0^{\perp})^2 = -\omega_0^2 + (5\alpha + 2\gamma) \psi_0 - 2e_a \eta_a, \quad (7)$$

Here, $\omega_0 \equiv \sqrt{v_0 - \kappa}$, is the frequency of a purely harmonic model where $v_0 \equiv C^2/3$ is the largest Fourier component of the dipole interaction; $\psi_0 = (2\omega)^{-1} \coth(\beta\omega/2)$ are local fluctuations of polarization with $\omega = \sqrt{(\Omega_0^{\perp})^2 + v_0}$ and $\eta_a = \langle \eta_1 + \eta_2 + \eta_3 \rangle = (e_a/C_a) (3\psi_0) + \sigma/C_a$ is the volume strain. $\langle \dots \rangle$ denotes thermal average.

Note that the largest contributions to λ come from the critical TO modes as the LO modes are gaped by the large depolarizing field, see Eq. (6).

We now parametrize the tunneling barrier energy between equivalent FE ground states with the Fermi energy and cation substitution.³ For displacive systems, it follows the Curie-Weiss temperature $T_{fe} \propto \omega_0$,³³ therefore we choose the following parametrization,

$$\omega_0^2 \rightarrow \omega_0^2 \left[1 - b_2 \left(e^{\epsilon_F/b_1} - 1 \right) - g(x_r - x) \right], \quad (8)$$

where ϵ_F is the Fermi level and x is the Ca concentration. $x_r = 0.018$ is the Ca concentration above which $\text{Sr}_{1-x}\text{Ca}_x\text{TiO}_3$ enters a glassy phase which we do not aim to describe here.^{28,38,39} b_1, b_2, g are model parameters that will be fitted to experiments. While this parametrization gives a monotonous hardening of the TO modes with carrier density as found by ab-initio calculations³ and experiments⁴⁰, it differs in its form from that of Edge et al.³ We find that this is necessary to simultaneously generate physically reasonable FE transition temperatures, phonon frequencies, and SC domes at the observed doping levels.

Equations (2), and (5)-(8) are a self-consistent system that give $T_c(n, \sigma)$, $T_{fe}(n, \sigma)$, and $\Omega_{01}^\perp(n, \sigma, T)$.

B. Ferroelectric phase

The observed FE order in STO:Ca has orthorhombic symmetry.²⁸ Such states, however, appear as saddle points in the free energy of the the Hamiltonian (3).⁴¹ Thus, we will assume that the FE ground state has a non-centrosymmetric tetragonal symmetry. In such phase, the two-fold degeneracy of the PE TO phonon is lifted and gives rise to two distinct modes Ω_{01}^\perp and Ω_{03}^\perp . There is also one LO frequency $\Omega_{01}^\perp + 3a_3$. According to Eq. (1), we therefore have,

$$\lambda(T_c, \sigma) = \alpha_{e-ph}^2 \sum_{\mathbf{q}} \left(\frac{1}{\Omega_{\mathbf{q}1}} + \frac{1}{\Omega_{\mathbf{q}2}} + \frac{1}{\Omega_{\mathbf{q}3}} \right), \quad (9)$$

where,³⁷

$$(\Omega_{\mathbf{q}1})^2 = (\Omega_{01}^\perp)^2 + B^2 |\mathbf{q}|^2, \quad (10a)$$

$$(\Omega_{\mathbf{q}2})^2 = (\Omega_{01}^\perp)^2 + B^2 |\mathbf{q}|^2 + \left[(\Omega_{03}^\perp)^2 - (\Omega_{01}^\perp)^2 \right] \left(\frac{q_\perp}{|\mathbf{q}|} \right)^2, \quad (10b)$$

$$(\Omega_{\mathbf{q}3})^2 = (\Omega_{01}^\perp)^2 + B^2 |\mathbf{q}|^2 + C^2 + \left[(\Omega_{03}^\perp)^2 - (\Omega_{01}^\perp)^2 \right] \left(\frac{q_z}{|\mathbf{q}|} \right)^2, \quad (10c)$$

where $q_\perp^2 = q_x^2 + q_y^2$. A is an order parameter which we have assumed to be along the c-axis of the tetragonal cell.

$\Omega_{01}^\perp, \Omega_{03}^\perp$, and A are given as follows,³⁴

$$(\Omega_{01}^\perp)^2 = \gamma A^2 + (2\alpha - \gamma) (\psi_1 - \psi_3) + 6e_t \eta_t, \quad (11a)$$

$$(\Omega_{03}^\perp)^2 = 2\alpha A^2, \quad (11b)$$

$$(\Omega_{03}^\perp)^2 = -\omega_0^2 + 3\alpha (A^2 + \psi_3) + 2(\alpha + \gamma) \psi_1 - 2e_a \eta_a - 4e_t \eta_t. \quad (11c)$$

$\psi_{1,3} = (2\omega_{1,3})^{-1} \coth(\beta\omega_{1,3}/2)$ are local fluctuations of polarization with $\omega_{1,3} = \sqrt{(\Omega_{01,3}^\perp)^2 + v_0}$, $\eta_a = \langle \eta_1 + \eta_2 + \eta_3 \rangle = (e_a/C_a) (2\psi_1 + A^2 + \psi_3) + \sigma/C_a$, and $\eta_t = \langle \eta_3 - \eta_1 \rangle = (3e_t/2C_t) (A^2 + \psi_3 - \psi_1)$ are volume and shear strains, respectively.

We assume the same parameterization for the tunneling barrier as that of the non-polar phase. Thus, Eqs. (2), and (8)-(11) give the relevant transition temperatures, phonon frequencies, and order parameter in a self-consistent fashion.

III. RESULTS AND DISCUSSION

The model parameters are given in Table I. $\omega_0, \alpha, \gamma, B, C, Q, e_a$, and e_t are obtained by fitting to the observed phonon frequencies,^{2,25,42} FE phase diagram,²⁸ and Debye temperature,¹⁷ of STO:Ca without doping. The elastic constants were taken from Ref. [43]. Typical results are shown in Fig. 1 and reproduce well the observed behavior. The parameters b_1, b_2 and α_{e-ph} are chosen to match the observed QCP in n-doped STO:Ca-0.9% at $n \simeq 0.2 \times 10^{20} \text{ cm}^{-3}$ ² and the maximum T_c ($\simeq 0.3 \text{ K}$) for n-doped STO without stress.⁸

We first discuss our results for applied stresses. Figure 2 (a) shows the calculated superconducting domes upon application of homogeneous stresses. In the absence of stresses, the dome is shown by the dashed line. Hydrostatic compression pushes the system away from the QCP by hardening the frequency of the TO phonons, therefore reducing the coupling constant as well as T_c . This is in qualitative agreement with experiments.^{4,5} Tensile stress, on the other hand, brings the system closer to the QCP by softening the phonons, therefore increasing the coupling constant and favoring superconductivity. For moderate stresses, inversion symmetry is broken, and a kink shows in T_c at the underlying QCP that occurs at same doping level. Optimal doping occurs at higher charge densities though. This is due to dimensionality alone, as we have found a similar result by replacing the dipolar-force with a short-range interaction. For large stresses, the dome becomes peaked and its maximum is pinned to the QCP. This behavior is in contrast with order-disorder models where the dome broadens and a sharp peak occurs at any strain-induced QCP.³²

We note that the trends in T_c depend crucially on the sign of the coupling constant e_a between the order parameter and the volume strain: for $e_a < 0$, T_c

would decrease with tensile stress. Such behavior would be observed in a hypothetical superconductor where the pairing is due to zone-boundary antiferrodistortive fluctuations.

Figure 2 (b) shows the phase diagram for doped STO under a fixed tensile stress ($\sigma/C_a = 0.51$) together with the quantum critical fan given by $\Omega < T \ll T_D$.³⁰ When approaching the QCP from the FE side, T_c is lower than without tensile stress (see dashed line in Fig. 2 (a)) and viceversa when the fluctuations become critical. We note that the quantum criticality extends over a narrow doping range. This is due to the long-range character of the dipolar force and the lattice dimensionality: both suppress the thermal and quantum fluctuations compared to one-dimensional models with short-range interactions.^{31,32}

Similar results are obtained when the QCP is approached by cation substitution. Figure 2 (c) shows the superconducting domes for several Ca concentrations displaying a kink and a peak for moderate and strong x , respectively. Figure 2 (d) shows the phase diagram for $x = 0.9\%$. We find again that, when compared to pure STO, T_c increases within the QC fan and decreases outside of it from the FE side. When comparing to recent experiments in n-doped STO:Ca and isotopic substituted STO,² our model suggests that the observed increase in T_c is due to pairs crossing-over to the QC fan.

IV. CONCLUSIONS

In summary, we have theoretically studied the effects of lattice dimensionality, long-range and anisotropic dipolar

forces, and strain coupling on the superconducting phase of STO by combining a standard model for displacive FEs with a strong-theory of superconductivity. We have shown that they unpin the maximum T_c from the QCP and restrict quantum criticality to a narrow doping window in which T_c is enhanced.

Our model gives a superconducting dome that is narrower than the observed one.^{7,15,44} This is a consequence of our parametrization of the tunneling barrier with the Fermi level given by Eq. (8) and for which a theory is clearly needed. We expect, however, that our main results to hold at a qualitative level. We have also neglected the effects of band-narrowing due to polaron formation, which could have strong effects on the correlations.^{45–50}

The theoretical framework presented here and its extensions could provide insight into the intriguing role of spatial inversion symmetry breaking in two-dimensional superconductivity at the interface of STO-based heterostructures,^{51,52} FeSe monolayers on STO,⁵³ as well as possible pairing mechanisms with new collective excitations originated by multiferroic QCPs.^{54,55}

V. ACKNOWLEDGMENTS

Work at the University of Costa Rica is supported by the Vice-rectory for Research under the project no. 816-B7-601, and work at Argonne National Laboratory is supported by the U.S. Department of Energy, Office of Basic Energy Sciences, Material Sciences and Engineering Division under contract no. DE-AC02-06CH11357.

-
- ¹ A. Stucky, G. W. Scheerer, Z. Ren, D. Jaccard, J.-M. Pomirol, C. Barreateau, E. Giannini, and D. van der Marel, “Isotope effect in superconducting n-doped SrTiO₃,” *Sci. Rep.* **6**, 37582 (2016).
 - ² C. W. Rischau, X. Lin, C. P. Grams, D. Finck, S. Harms, J. Engelmayer, T. Lorenz, Y. Gallais, B. Fauque, J. Hemberger, and K. Behnia, “A ferroelectric quantum phase transition inside the superconducting dome of Sr_{1-x}Ca_xTiO_{3-δ},” *Nat. Phys.* **13**, 643–648 (2017).
 - ³ J. M. Edge, Y. Kedem, U. Aschauer, N. A. Spaldin, and A. V. Balatsky, “Quantum critical origin of the superconducting dome in SrTiO₃,” *Phys. Rev. Lett.* **115**, 247002 (2015).
 - ⁴ S. E. Rowley, C. Enderlein, J. Ferreira de Oliveira, D. A. Tompsett, E. Baggio Saitovitch, S. S. Saxena, and G. G. Lonzarich, “Superconductivity in the vicinity of a ferroelectric quantum phase transition,” *arXiv:1801.08121* (2018).
 - ⁵ E. R. Pfeiffer and J. F. Schooley, “Effect of stress on the superconducting transition temperature of SrTiO₃,” *J. Low Temp. Phys.* **2**, 333–352 (1970).
 - ⁶ J. F. Schooley, W. R. Hosler, and M. L. Cohen, “Superconductivity in semiconducting SrTiO₃,” *Phys.*

- Rev. Lett.* **12**, 474–475 (1964).
- ⁷ J. F. Schooley, W. R. Hosler, E. Ambler, J. H. Becker, M. L. Cohen, and C. S. Koonce, “Dependence of the superconducting transition temperature on carrier concentration in semiconducting SrTiO₃,” *Phys. Rev. Lett.* **14**, 305 (1965).
- ⁸ C. S. Koonce, M. L. Cohen, J. F. Schooley, W. R. Hosler, and E. R. Pfeiffer, “Superconducting transition temperatures of semiconducting SrTiO₃,” *Phys. Rev.* **163**, 380–390 (1967).
- ⁹ G. Binnig, A. Baratoff, H. E. Hoenig, and J. G. Bednorz, “Two-band superconductivity in Nb-doped SrTiO₃,” *Phys. Rev. Lett.* **45**, 1352 (1980).
- ¹⁰ Hiroshi Suzuki, Hiroshi Bando, Youiti Ootuka, Isao H. Inoue, Tetsuya Yamamoto, Kazuhiko Takahashi, and Yoshikazu Nishihara, “Superconductivity in single-crystalline Sr_{1-x}La_xTiO₃,” *J. Phys. Soc. Jpn.* **65**, 1529–1532 (1996).
- ¹¹ D.M. Eagles, “Superconductivity at very low carrier concentrations and indications of a charged bose gas in SrTi_{0.97}Zr_{0.03}O₃,” *Solid State Comm.* **60**, 521–524 (1986).
- ¹² D.M. Eagles, R.J. Tainsh, and C. Andrikidis, “Evidence for pairing without superconductivity from resistance

- between 130 mK and 70 mK in a specimen of ceramic Zr-doped SrTiO₃,” *Physica C: Superconductivity* **157**, 48 – 52 (1989).
- 13 R.J. Tainsh and C. Andrikidis, “Superconducting transitions from states with low normal conductivity in ceramic SrTi_{0.97}Zr_{0.03}O₃,” *Solid State Comm-* **60**, 517 – 519 (1986).
 - 14 D. M. Eagles, “Comment on two papers claiming records for the lowest carrier concentration at which superconductivity has been observed,” [arXiv:1604.05660](https://arxiv.org/abs/1604.05660) (2016).
 - 15 X. Lin, Z. Zhu, B. Fauqué, and K. Behnia, “Fermi surface of the most dilute superconductor,” *Phys. Rev. X* **3**, 021002 (2013).
 - 16 J. P. Carbotte, “Properties of boson-exchange superconductors,” *Rev. Mod. Phys.* **62**, 1027–1157 (1990).
 - 17 G. Burns, “Comment on the low temperature specific heat of ferroelectrics, antiferroelectrics, and related materials,” *Solid State Comm.* **35**, 811 – 814 (1980).
 - 18 L. P. Gor’kov, “Phonon mechanism in the most dilute superconductor n-type SrTiO₃,” *Proc. Natl. Acad. Sci.* **113**, 4646–4651 (2016).
 - 19 J. Ruhman and P. A. Lee, “Superconductivity at very low density: the case of strontium titanate,” *Phys. Rev. B* **94**, 224515 (2016).
 - 20 Y. Takada, “Theory of superconductivity in polar semiconductors and its application to n-type semiconducting SrTiO₃,” *J. Phys. Soc. Jpn.* **49**, 1267–1275 (1980).
 - 21 D M Broun, “What lies beneath the dome?” *Nat. Phys.* **4**, 170 (2008).
 - 22 M. Vojta, “Quantum phase transitions,” *Rep. Prog. Phys.* **66**, 2069 (2003).
 - 23 A. G. Swartz, H. Inoue, T. A. Merz, Y. Hikita, S. Raghu, T. P. Devereaux, S. Johnston, and H. Y. Hwang, “Polaronic behavior in a weak coupling superconductor,” [arXiv:1608.05621](https://arxiv.org/abs/1608.05621) (2016).
 - 24 K. A. Müller and H. Burkard, “SrTiO₃: An intrinsic quantum paraelectric below 4 K,” *Phys. Rev. B* **19**, 3593–3602 (1979).
 - 25 Y. Yamada and G. Shirane, “Neutron scattering and nature of the soft optical phonon in SrTiO₃,” *J. Phys. Soc. Jpn.* **26**, 396–403 (1969).
 - 26 E. L. Venturini, G. A. Samara, M. Itoh, and R. Wang, “Pressure as a probe of the physics of ¹⁸O-substituted SrTiO₃,” *Phys. Rev. B* **69**, 184105 (2004).
 - 27 M. Itoh, R. Wang, Y. Inaguma, T. Yamaguchi, Y-J. Shan, and T. Nakamura, “Ferroelectricity induced by oxygen isotope exchange in strontium titanate perovskite,” *Phys. Rev. Lett.* **82**, 3540–3543 (1999).
 - 28 J. G. Bednorz and K. A. Müller, “Sr_{1-x}Ca_xTiO₃: An xy quantum ferroelectric with transition to randomness,” *Phys. Rev. Lett.* **52**, 2289–2292 (1984).
 - 29 P. Chandra, G. G. Lonzarich, S. E. Rowley, and J. F. Scott, “Prospects and applications near ferroelectric quantum phase transitions,” *Rep. Prog. Phys.* **80**, 112502 (2017).
 - 30 S. E. Rowley, L. J. Spalek, R. P. Smith, M. P. M. Dean, M. Itoh, J. F. Scott, G. G. Lonzarich, and S. S. Saxena, “Ferroelectric quantum criticality,” *Nat. Phys.* **10**, 367–372 (2014).
 - 31 Y. Kedem, J.-X. Zhu, and A. V. Balatsky, “Unusual superconducting isotope effect in the presence of a quantum criticality,” *Phys. Rev. B* **93**, 184507 (2016).
 - 32 K. Dunnett, A. Narayan, N. A. Spaldin, and A. V. Balatsky, “Strain and ferroelectric soft mode induced superconductivity in strontium titanate,” [arXiv:1712.08368](https://arxiv.org/abs/1712.08368) (2017).
 - 33 M. E. Lines and A. M. Glass, *Principles and Applications of Ferroelectrics and Related Materials* (Oxford University Press, 2001).
 - 34 E. Pytte, “Theory of perovskite ferroelectrics,” *Phys. Rev. B* **5**, 3758 (1972).
 - 35 W. L. McMillan, “Transition temperature of strongly-coupled superconductors,” *Phys. Rev.* **167**, 331–344 (1968).
 - 36 A. Aharony and M. E. Fisher, “Critical behavior of magnets with dipolar interactions. i. renormalization group near four dimensions,” *Phys. Rev. B* **8**, 3323 (1973).
 - 37 J. R. Arce-Gamboa and G. G. Guzmán-Verri, “Random electric field instabilities of relaxor ferroelectrics,” *npj Quantum Materials* **2**, 28 (2017).
 - 38 W. Kleemann, F. J. Schäfer, K. A. Müller, and J. G. Bednorz, “Domain state properties of the random-field xy-model system Sr_{1-x}Ca_xTiO₃,” *Ferroelectrics* **80**, 297–300 (1988).
 - 39 W. Kleemann, A. Albertini, M. Kuss, and R. Lindner, “Optical detection of symmetry breaking on a nanoscale in SrTiO₃:Ca,” *Ferroelectrics* **203**, 57–74 (1997).
 - 40 D. Bäuerle, D. Wagner, M. Wöhlecke, B. Dorner, and H. Kraxenberger, “Soft modes in semiconducting SrTiO₃: II. the ferroelectric mode,” *Zeitschrift für Physik B Condensed Matter* **38**, 335–339 (1980).
 - 41 R. A. Cowley, “Structural phase transitions I. Landau theory,” *Adv. Phys.* **29**, 1 (1980).
 - 42 G. A. Samara, “The Grüneisen parameter of the soft ferroelectric mode in the cubic perovskites,” *Ferroelectrics* **2**, 177–182 (1971).
 - 43 M. Carpenter, “Elastic anomalies accompanying phase transitions in (Ca,Sr)TiO₃ perovskites: Part I. Landau theory and a calibration for SrTiO₃,” *Am. Mineral.* **92**, 309 (2007).
 - 44 M. Thiemann, M. H. Beutel, M. Dressel, N. R. Lee-Hone, D. M. Broun, E. Fillis-Tsirakis, H. Boschker, J. Mannhart, and M. Scheffler, “Single gap superconductivity in doped SrTiO₃,” [arXiv:1703.04716](https://arxiv.org/abs/1703.04716) (2017).
 - 45 M. Gabay and J.-M. Triscone, “Ferroelectricity woos pairing,” *Nat. Phys.* **13**, 624 (2017).
 - 46 Z. Wang, S. McKeown Walker, A. Tamai, Y. Wang, Z. Ristic, F. Y. Bruno, A. de la Torre, S. Riccò, N. C. Plumb, M. Shi, P. Hlawenka, J. Sánchez-Barriga, A. Varykhalov, T. K. Kim, M. Hoesch, P. D. C. King, W. Meevasana, U. Diebold, J. Mesot, B. Moritz, T. P. Devereaux, M. Radovic, and F. Baumberger, “Tailoring the nature and strength of electron-phonon interactions in the SrTiO₃(001) 2D electron liquid,” *Nat. Mat.* **3**, 1–6 (2016).
 - 47 D. van der Marel, J. L. M. van Mechelen, and I. I. Mazin, “Common Fermi-liquid origin of T^2 resistivity and superconductivity in n-type SrTiO₃,” *Phys. Rev. B* **84**, 205111 (2011).
 - 48 J. T. Devreese, S. N. Klimin, J. L. M. van Mechelen, and D. van der Marel, “Many-body large polaron optical conductivity in SrTi_{1-x}Nb_xO₃,” *Phys. Rev. B* **81**, 125119 (2010).
 - 49 W. Meevasana, X. J. Zhou, B. Moritz, C-C. Chen, R. H. He, S-I. Fujimori, D. H. Lu, S-K. Mo, R. G. Moore,

- F. Baumberger, T. P. Devereaux, D. van der Marel, N. Nagaosa, J. Zaanen, and Z-X. Shen, "Strong energy-momentum dispersion of phonon-dressed carriers in the lightly doped band insulator SrTiO₃," *New J. Phys.* **12**, 023004 (2010).
- ⁵⁰ J. L. M. van Mechelen, D. van der Marel, C. Grimaldi, A. B. Kuzmenko, N. P. Armitage, N. Reyren, H. Hagemann, and I. I. Mazin, "Electron-phonon interaction and charge carrier mass enhancement in SrTiO₃," *Phys. Rev. Lett.* **100**, 226403 (2008).
- ⁵¹ S. Gariglio, M. Gabay, and J.-M. Triscone, "Research update: conductivity and beyond at the LaAlO₃/SrTiO₃ interface," *APL Materials* **4**, 060701 (2016).
- ⁵² Y.-Y. Pai, A. Tylan-Tyler, P. Irwin, and J. Levy, "Prospects and applications near ferroelectric quantum phase transitions," *Rep. Prog. Phys.*, in press (2018).
- ⁵³ J. J. Lee, F. T. Schmitt, R. G. Moore, S. Johnston, Y.-T. Cui, W. Li, M. Yi, Z. K. Liu, M. Hashimoto, Y. Zhang, D. H. Lu, T. P. Devereaux, D.-H. Lee, and Z.-X. Shen, "Interfacial mode coupling as the origin of the enhancement of T_c in FeSe films on SrTiO₃," *Nature* **515**, 245 (2014).
- ⁵⁴ C. Morice, P. Chandra, S. E. Rowley, G. Lonzarich, and S. S. Saxena, "Hidden fluctuations close to a quantum bicritical point," *Phys. Rev. B* **96**, 245104 (2017).
- ⁵⁵ A. Narayan, A. V. Balatsky, and N. A. Spaldin, "Multiferroic quantum criticality," *arXiv:1711.07989* (2017).